ACS APPLIED MATERIALS & INTERFACES

Research Article

www.acsami.org

Three-Dimensional Cobalt Oxide Microstructures with Brush-like Morphology via Surfactant-Dependent Assembly

Duc Tai Dam and Jong-Min Lee*

School of Chemical and Biomedical Engineering, Nanyang Technological University, Singapore 637459, Singapore

Supporting Information

ABSTRACT: In this study, three-dimensional cobalt oxide microstructures were developed. Cobalt oxide microdumbbells and microspheres, assembled by nanowires and primary particles, were successfully synthesized by a multistep hydrothermal method. Of all of the structures, the cobalt oxide microdumbbell electrode possesses the largest surface area of 70.8 m^2 g^{-1} and the highest specific capacitance of 407.5 F g^{-1}. The as-prepared electrode also demonstrates excellent electrochemical stability and retains 97.5% of the initial capacitance after 2000 charge−discharge cycles. This performance is attributed to the desirable morphology, uniform microarchitecture stability, and high surface area. The results show that the as-fabricated Co_3O_4 is a promising electrode material for supercapacitor applications.

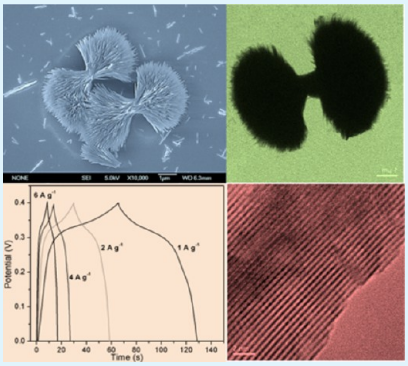

KEYWORDS: *supercapacitor, cobalt oxide, hydrothermal, microdumbbell, electrochemical, hexanitrocobaltate*

INTRODUCTION

Over the last decade, pseudocapacitors or supercapacitors, which capture and release electrons through reversible faradaic reactions on the interface between active material and electrolyte, have drawn considerable attention. This is owing to their outstanding properties such as high power density, low fabrication cost, rapid energy charging, and excellent cycle life.[1,2] Of all electrode materials, hydrated ruthenium oxide with high conductivity and three distinct oxidation states exhibits high specific capacitance.[3] However, despite all of the above advantages, ruthenium-based electrochemical capacitors are still not widely commercialized due to their high cost, limited ruthenium resources, and their toxic nature. Therefore, it is essential to develop alternative low-cost electrode materials. Transition metal hydroxides/oxides including cobalt hydroxide,[4,5] cobalt oxide,[6,7] nickel oxide,[8,9] manganese oxide,[10−12] and their composites[13−15] are promising candidates for the next generation of redox materials in pseudocapacitors. Among the potential candidates, cobalt-based hydroxide and oxide are of particular interest due to their well-defined redox activity, great reaction reversibility, and cost-effectiveness.

It is commonly postulated that the electrochemical performance of electrode nanostructures depend on their surface area, particles size, crystal structure, and morphology. With the aim to increase active surface area, tremendous efforts have been devoted to fabricating nanostructures with different and controlled shapes such as nanowires,[16−18] nanosheets,[19,20] nanotubes,[21,22] and hollow particles.[23,24] These studies focused on high activities of nanosized materials/structures to improve the electrochemical behavior of supercapacitor electrode materials. From our point of view, most of the reports were more concerned about the initial capacitance, but inadequate attention was paid to the electrochemical stability during charge/discharge cycles. On the other hand, recent studies[6,25−27] also show that stable three-dimensional (3D) microstructures of nanobuilding blocks are highly desirable for achieving enhanced electron transport, improved ionic diffusion, excellent rate capability, and great stability. Therefore, it is imperative to develop systematic and rational techniques to fabricate electrode materials with well-defined microstructures containing advantageous properties. On top of that, this intriguing approach can be potentially adopted to widely synthesize supercapacitor electrode materials with better electrochemical performance to meet rising energy demand in the near future.

A common approach to prepare metal oxides is through the thermal decomposition of a metal precursor obtained by hydrothermal or sol−gel methods. A similar strategy can be utilized to synthesize pseudocapacitive cobalt oxide (Co_3O_4). Two popular precursors are cobalt hydroxide and cobalt carbonate. They are good due to their ease of synthesis and stability at high temperatures in hydrothermal conditions. In the synthesis of microstructures under hydrothermal conditions, sodium carbonate,[28] urea,[29−31] and glucose[24,32] are usually utilized as carbon sources or precipitating reagents/additives. However, the additives are generally not desirable in the synthesis due to difficulties in consistent control of morphology and particle size.

Received: July 15, 2014
Accepted: November 12, 2014
Published: November 21, 2014

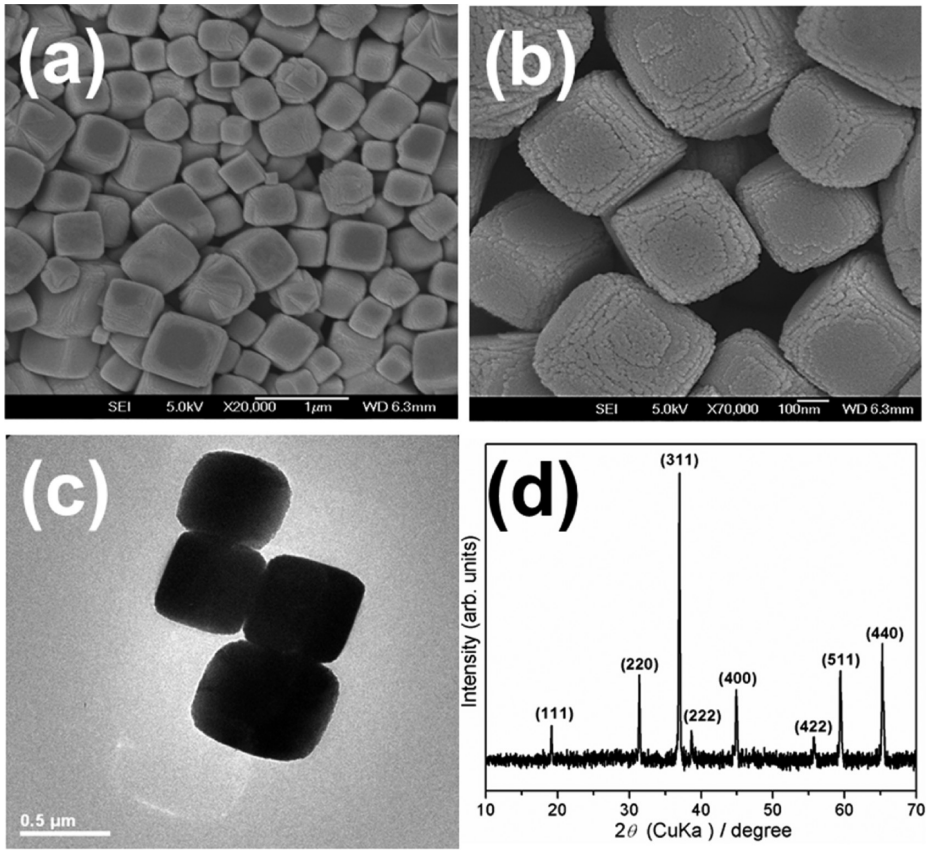

Figure 1. (a and b) Field-emission SEM (FESEM) images (c) TEM image (d) XRD pattern of Co_3O_4 nanocubes.

Thus, in this study, we demonstrated a facile and scalable technique, in which a cobalt precursor can be produced from hexanitrocobaltate complex as a cobalt source without addition of the above reagents. We prepared a three-dimensional (3D) brush-like cobalt oxide with tunable shape transformation from microsphere to microdumbbell. A hydrothermal method was carried out to synthesize cobalt carbonate hydroxide, followed by calcination to obtain cobalt oxide microarchitecture. Interestingly, we found out that the addition of cobalt oxide nanocubes into the reaction mixture was responsible for the transformation from a spherical shape to dumbbell architecture. The use of polyvinylpyrrolidone also improves the uniformity of the as-prepared microdumbbells. A series of hydrothermal reactions in chronological order were performed to study the formation mechanism of the cobalt precursor with brush-like morphology. We also carefully investigated electrochemical properties of the as-prepared hierarchical 3D structure in a 6 M KOH electrolyte solution. The as-prepared microdumbbells and microspheres exhibit specific capacitances of 407.5 and 350.9 F g^{-1}, respectively. In addition, both electrode materials (i.e., microdumbbell and microsphere) can preserve more than 96% of their initial capacitances after 2000 charge−discharge cycles.

RESULTS AND DISCUSSION

Co_3O_4 nanocubes were synthesized by a hydrothermal method with $Na_3Co(NO_2)_6$ as a source of cobalt in a solvent mixture of deionized (DI) water and ethanol in a 25 mL polytetrafluoroethylene (PTFE) Teflon-lined autoclave at 150 °C for 12. To characterize the Co_3O_4 nanocubes formed in the mixture of water and ethanol, X-ray diffraction (XRD), scanning electron microscopy (SEM), and transmission electron microscopy (TEM) were used. The results are shown in Figure 1. The low-magnification SEM image (Figure 1a) and the TEM image (Figure 1c) show the successful synthesis of nanocubes with a side dimension of c.a. 300−500 nm. The high-magnification SEM image (Figure 1b) indicates that nanocubes have rough surfaces consisting of many primary nanoparticles. The nanocube solids extracted from the solvent mixture appeared dark black. On top of that, the XRD pattern (Figure 1d) can also be attributed to cobalt oxide (Co_3O_4) without secondary phases/impurities.

The formation of the Co_3O_4 nanocubes is likely due to the hydrolysis of the hexanitrocobaltate anion in a neutral medium and the conversion of unstable intermediates to more stable Co_3O_4. Rakhi and his colleagues reported similar phenomenon.[6] The mechanism of formation probably proceeds through a series of reactions as follows

$$CH_3CH_2OH + H_2O \rightarrow CH_3CH_2OH_2^+ + OH^- \quad (1)$$

$$Co(NO_2)_6^{3-}(aq) \rightarrow Co^{3+}(aq) + 6NO_2^- \quad (2)$$

$$Co^{3+} + 3OH^- \rightarrow Co(OH)_3 \rightarrow CoOOH \rightarrow Co_3O_4 \quad (3)$$

The cobalt precursors with different shapes, microspheres, and microdumbbells, were prepared in water/ethylene glycol mixtures, which also contain a hexanitrocobaltate anion with or without Co_3O_4 added, respectively. In an attempt to gain insight into the formation of the cobalt precursors, their morphology and crystal structures were investigated. Microparticles with two typical shapes of spheres and dumbbells were observed in low-magnification FESEM images in Figure 2a,c.

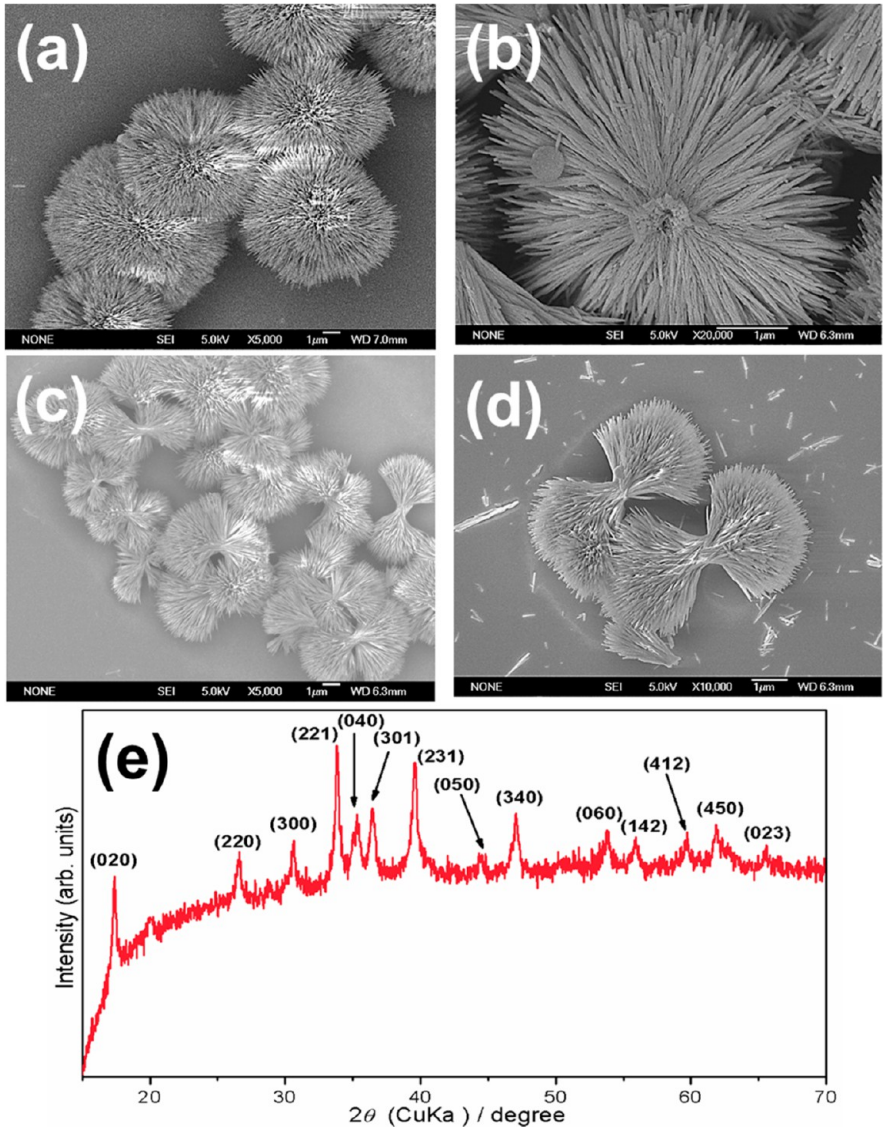

Figure 2. (a and b) FESEM images of $Co_2(CO_3)(OH)_2{\cdot}0.22H_2O$ microspheres. (c and d) FESEM images of $Co_2(CO_3)(OH)_2{\cdot}0.22H_2O$ microdumbbells. (e) XRD pattern of cobalt carbonate hydroxide hydrate.

The magnified FESEM images (Figure 2b,d) clearly show two different structures and indicates that the surfaces of microstructures were constructed by agglomeration of nanowires, forming a brush-like morphology. The diameters of the cobalt precursors are around 3−5 μm. Even though two different experimental procedures were adopted, identical cobalt precursors with similar crystal structures were generated and confirmed to be $Co_2(CO_3)(OH)_2{\cdot}0.22H_2O$ (JCPDS No. 48-0083) by XRD measurement (Figure 2e). Thermal analysis was carried out to investigate thermal stability of the as-prepared cobalt-based precursor. The TGA curve of the cobalt carbonate hydroxide precursor is presented in Figure S1 (Supporting Information). On the basis of the TGA analysis, the cobalt carbonate hydroxide hydrate was calcined at 300 °C for 2 h to ensure complete conversion to Co_3O_4 and achieve high crystallinity.

TEM characterization was also performed to study particularly the crystal structure of the as-synthesized cobalt precursors. Figure 3a,b shows needle-like nanowires growing from inside out, forming the urchin surface. The architecture consists of plenty of nanowires having a diameter in the range of 30−40 nm. The individual nanowires were studied by a high-resolution TEM (HRTEM, Figure 3c). All of them exhibit uniform lattice fringes. A lattice-resolved HRTEM image of a representative nanowire indicates that the nanowires of the cobalt precursor are single-crystalline without any amorphous phases. The lattice spacing is about 0.44 nm corresponding to (001) planes (JCPDS No. 48-0083). As such, the growth direction is parallel to this vertical lattice orientation. Therefore, the nanowires preferably grow along the [100] direction. The single crystallinity is confirmed by the diffraction pattern (SAED) measurement of a selected area, presented in Figure 3d.

The cobalt carbonate hydroxide microsphere with brush-like morphology can be formed easily by the one-step hydrothermal technique without surfactant. No precursor was generated when ethylene glycol was withheld to the solution mixture and no other cobalt salts were used. This phenomenon indicates the importance of nitrite ligands (NO_2^-) and ethylene glycol in the precipitation of the cobalt(II) precursor. The reaction might proceed as follows

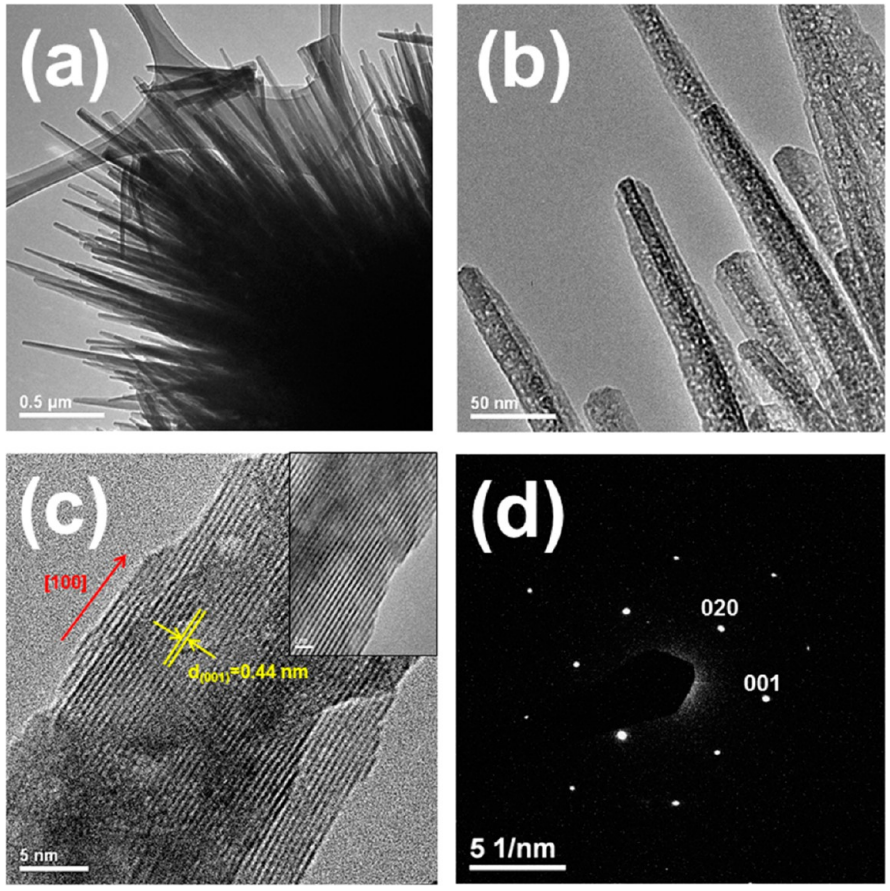

Figure 3. (a and b) Low-magnification TEM images of $Co_2(CO_3)(OH)_2{\cdot}0.22H_2O$ nanowire bundle, (c) HRTEM image of a $Co_2(CO_3)(OH)_2{\cdot}0.22H_2O$ nanowire, and (d) corresponding SAED of cobalt carbonate hydroxide precursors.

$$4Co^{3+} + C_2H_6O_2 + NO_2^- + 5.44H_2O + 2O_2 \rightarrow 2Co_2(CO_3)(OH)_2{\cdot}0.22H_2O + 12H^+ + NO_3^- \quad (4)$$

This is the first case that demonstrates the synthesis of microdumbbells transformed from cobalt oxide nanocubes. Two-step solvothermal method was adopted to prepare Co_3O_4 nanocubes and its conversion to hierarchical dumbbell cobalt carbonate hydroxide. Again, the cobalt precursor could not be formed without the addition of ethylene glycol into the solvent mixture. This highlights the crucial role of ethylene glycol in redissolution of Co_3O_4 nanoparticle, anisotropic growth of nanowire along the [100] direction and final conversion to the brush-like cobalt precursor. The process might be elaborated via modified Ostwald ripening and Kirkendall effects with cobalt ions of different oxidation states as follows

$$4Co_3O_4 + 3C_2H_6O_2 + NO_2^- + 6O_2 \rightarrow 6Co_2(CO_3)(OH)_2{\cdot}0.22H_2O + NO_3^- + 1.68H_2O \quad (5)$$

The dissolution of the cobalt oxide and the progressive conversion to the cobalt carbonate hydroxide nanowire could be perceived as outward diffusion and condensation. This phenomenon can be attributed to the modified Ostwald ripening and Kirkendall effects. To investigate the effect of time, products at different reaction stages were collected and characterized. The as-prepared samples were characterized by FESEM and XRD. Structural changes are clearly observed in Figure 4. At the early stage of reaction (1.5 h), the nanocubes remain relatively intact in spite of a certain degree of peripheral etching. All the XRD peaks of the products retrieved at the stage can be attributed to Co_3O_4. At 3 h, we can observe the onset of the transformation of morphology. When reaction time is maintained at 3−6 h, dissolution of the core of the nanocube is clearly observed, which leads to the radial growth and splitting of the nanowire. Since the outward diffusion of cobalt (II, III) oxide at the core of the nanocube is faster than the inward diffusion of Co(III) ions, void spaces are formed between the first-generation nanowires. In the XRD spectrum of the product at 6 h, diffraction peaks of $Co_2(CO_3)(OH)_2$ start to appear at 2θ = 33.8° and 39.5°, which are assigned to two dominant planes of (221) and (231). Complete conversion was at the reaction time of 9−12 h. It was confirmed by the XRD characterization.

The final products of cobalt oxide spheres and dumbbells with hierarchical microstructures can be obtained by thermal annealing of the corresponding precursors at 300 °C for 2 h. The shape and morphology are retained upon heat treatment to thermally convert the cobalt precursor to cobalt oxide. This is clearly observed in the FESEM images at different magnifications (Figure 5a,b,c,d). On top of that, the high magnification images show that the nanowires become rougher and consist of numerous nanoparticles with irregular shapes. In other words, the 3D hierarchical architectures (i.e., brush-like microspheres and microdumbbells) were constructed by nanoparticles as primary building blocks. The complete conversion to Co_3O_4 was examined by XRD measurement. The result is shown in Figure 5e. Several diffraction peaks at 2θ = 19°, 31.2°, 36.8°,

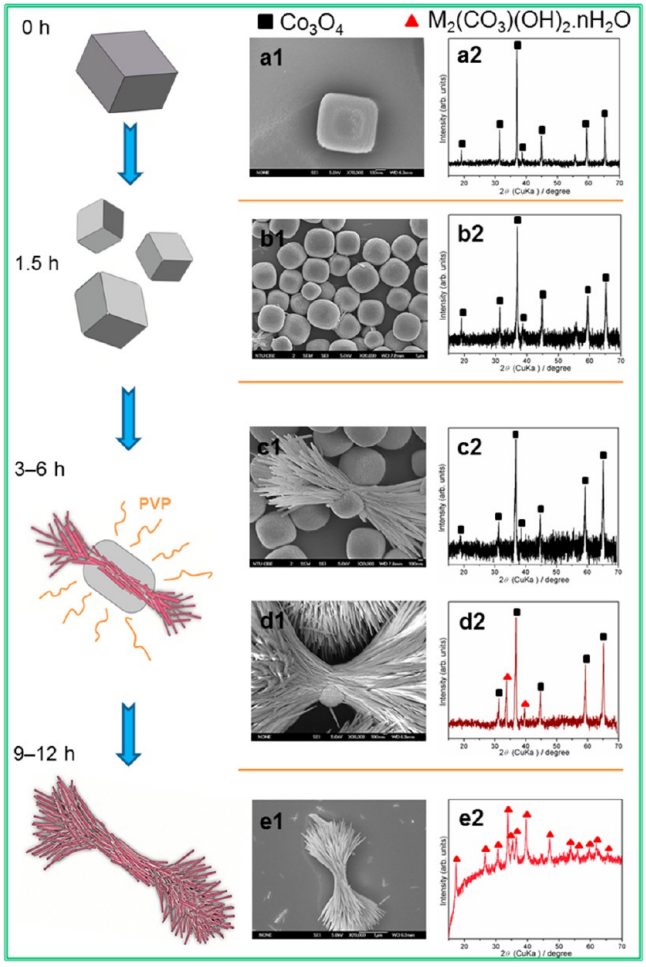

Figure 4. Illustrative schematic mechanism of the growth of cobalt precursor with dumbbell structure (a1, b1, c1, d1, e1) FESEM images, and (a2, b2, c2, d2, e2) XRD spectra of products obtained at different reaction times.

38.5°, 44. 8°, 55.7°, 59.4°, 65.2° correspond to the (111), (220), (311), (222), (400), (422), (511), (440) crystal planes of the cobalt oxide (Co_3O_4, JCPDS No. 42-1467), respectively. This result is also substantiated by Raman measurement, as presented in Figure 5f. The Raman spectrum comprises three major peaks at 472 cm^{-1} (E_g), 507 cm^{-1} (F_{2g}), and 662 cm^{-1} (A_{1g}), all of which are active vibrational modes of the Co_3O_4 crystalline phase.

TEM analysis also confirms successful thermal conversion to cobalt oxide without substantial change in morphology. Microstructure and nanostructure of the as-prepared cobalt oxide were studied, and the results are presented in Figure 6. Figure 6a,b shows low-magnification TEM images of the representative cobalt oxide microspheres and microdumbbells, respectively. TEM images of nanowire bundles (Figure 6c) and individual nanowires (Figure 6d) generated by intensive sonication illustrate the fact that thermal decomposition of the cobalt precursor is accompanied by release of gases and the formation of a porous structure. This type of porous structure is believed to be very beneficial to electrolyte diffusion and electron transport in supercapacitor applications. The HRTEM image (Figure 6e) of area indicated by the yellow square in Figure 6d shows some visible lattice fringes with interplanar distances of 0.46, 0.28, and 0.24 nm corresponding to the (111), (220), and (311) planes of polycrystalline Co_3O_4, as supported by its SAED analysis illustrated in Figure 6e.

Further pore structure characterization was also performed, shown in Figure S2, Supporting Information. The surface areas of cobalt oxide with different structures are derived from nitrogen adsorption/desorption isotherms and calculated to be 70.8, 60.7, and 4.1 $m^2\ g^{-1}$ for microdumbbell, microsphere, and nanocube structures, respectively. The larger surface area of the cobalt oxide microdumbbell is expected to result in better electrochemical performance than the other two structures. On the other hand, pore size distributions were determined from the desorption curve. Dumbbell and sphere microstructures have average pore sizes of 8.1 and 9.0 nm, respectively, indicating their mesoporous nature.

Electrochemical performances of the as-prepared materials were investigated by cyclic voltammogram (CV) and galvanostatic charge–discharge (chronopotentiometry) techniques in a 6 M KOH electrolyte. A supercapacitor electrode made of cobalt oxide stores energy mainly through reversible redox reactions as follows

$$Co_3O_4 + OH^- + H_2O \leftrightarrow 3CoOOH + e^- \quad (6)$$

,

Clear oxidation and reduction peaks are observed from the CV curves of three different Co_3O_4 structures at a scan rate of 10 mV s^{-1} (Figure 7a). CV measurements also allow us to confirm pseudocapacitive behaviors of the as-prepared electrodes which are clearly different from electrical double-layer capacitors (EDLCs) with a CV curve resembling ideal rectangular shape.[33,34] The area under the CV curve of the Co_3O_4 microdumbbell electrode is larger than those of the Co_3O_4 microsphere and the Co_3O_4 nanocube, indicating the superior supercapacitive performance of the Co_3O_4 microdumbbell as compared to the other two structures. Maximum specific capacitances of the Co_3O_4 microdumbbell, microsphere, and nanocube electrodes are derived from charge–discharge measurements at 1 A g^{-1} (Figure S3, Supporting Information) and determined to be 407.5, 350.9, and 246.6 F g^{-1}, respectively. From above measurements, conclusion can be drawn that pseudocapacitive properties of as-prepared products are morphology dependent. Similar finding was reported in[35] where the authors developed a facile strategy to synthesize hydrotalcite-like α-$Co(OH)_2$ as the precursor to generate Co_3O_4 with nanostructures. The main focus in this study was to tune interlayer chemistry and morphology of α-$Co(OH)_2$, which, in turn, resulted in significant enhancement in supercapacitive performance of Co_3O_4 nanostructure.

Rate capabilities of three types of electrodes were compared by measuring specific capacitance at different current densities in the range of 1–6 A g^{-1}. The result is shown in Figure S4 (Supporting Information). Taking the specific capacitance value at 1 A g^{-1} as original capacitance, Co_3O_4 microdumbbell electrode retained 100%, 90.9%, 83.6%, and 78.5% at 1, 2, 4, and 6 A g^{-1}, respectively. The Co_3O_4 microsphere exhibits comparable capacitance retention of 100%, 91.2%, 84.3%, and 77.5% at 1, 2, 4, and 6 A g^{-1}, respectively. Co_3O_4 nanocube demonstrates inferior capacitance retention of 100%, 86%, 77.3%, and 69.5% at 1, 2, 4, and 6 A g^{-1}, respectively.

Figure 7b represents the CV curves of the Co_3O_4 microdumbbell electrode at various scan rates in the range of 10–200 mV s^{-1}. The increasing scan rate is accompanied by increasing peak separations and peak currents. As an attempt to quantify specific capacitance of the as-prepared Co_3O_4

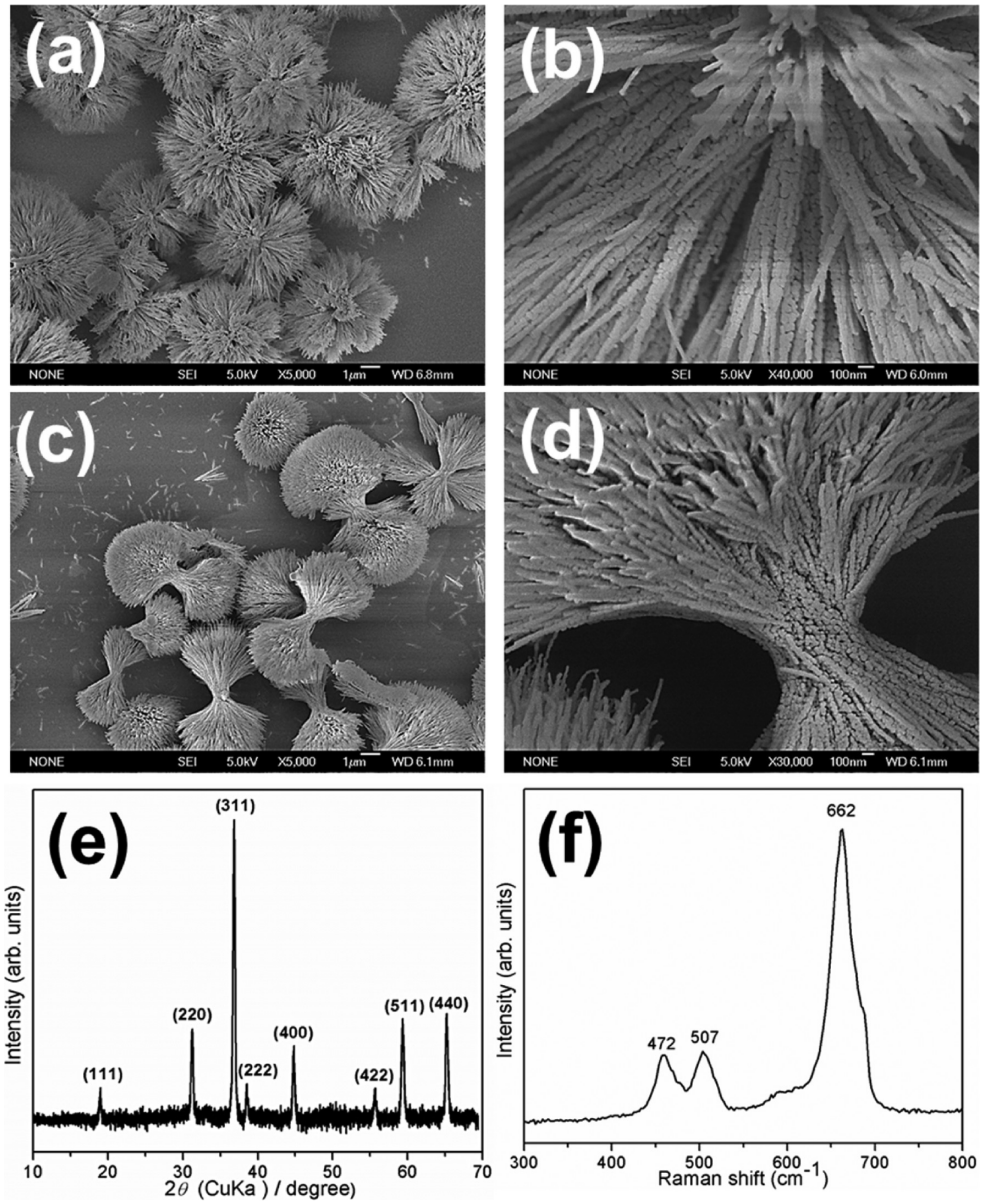

Figure 5. FESEM images of (a and b) microspheres, (c and d) microdumbbells obtained after calcination of cobalt precursors at 300 °C for 2 h. (e) XRD spectrum and (f) Raman pattern of cobalt oxide.

microdumbbell structure, chronopotentiometry was carried out at various current densities in a potential window of −0.1−+0.4 V in 6 M KOH solution (Figure 7c). The specific capacitances are estimated to be 407.5, 370.5, 340.8, and 320.1 F g^{-1} at current densities of 1, 2, 4, and 6 A g^{-1}, respectively. On top of that, the symmetric semitriangular shapes in the typical charge−discharge process at the current densities suggest stable pseudocapacitive behavior of the electrode.[24]

Cycling performance is one key factor that allows supercapacitors to be widely used in various applications. Therefore, charge−discharge cycling tests were carried out to study cycle life of the as-fabricated electrodes. The cycling tests were performed at 1 A g^{-1} for 2000 cycles. As presented by Figure 7d, the Co_3O_4 microdumbbell and microsphere electrodes exhibit excellent cycle and can retain 97.5% and 96.8% of their initial capacitance, respectively. The results indicate that the as-prepared materials are promising candidates for supercapacitor electrode materials. However, Co_3O_4 nanocubes demonstrate a lower retention percentage of only 83.9%. Nanostructures have high surface area and good capacitance but suffer from inadequate stability in the first 1000 cycles.[4,8,14] This drawback is likely due to distortion of morphology and small particle size. In order to overcome this issue, we purposely designed microstructures of tunable shapes to enhance the electrochemical stability of supercapacitor electrode. The high stability of Co_3O_4 dumbbells and spheres in alkaline solution can be attributed to three-dimensional (3D) microstructures of nanobuilding blocks.

Electrochemical impedance measurements were carried out in with the amplitude of the perturbation signal equal to 50 mV to measure electrode resistance and electrolyte diffusion. The results are presented in Figure 8. A typical electrochemical impedance spectroscopy (EIS) curve is composed of two main components: the semicircular loop at high frequencies representing charge-transfer resistance of the electrode and the straight segment at lower frequencies describing capacitive

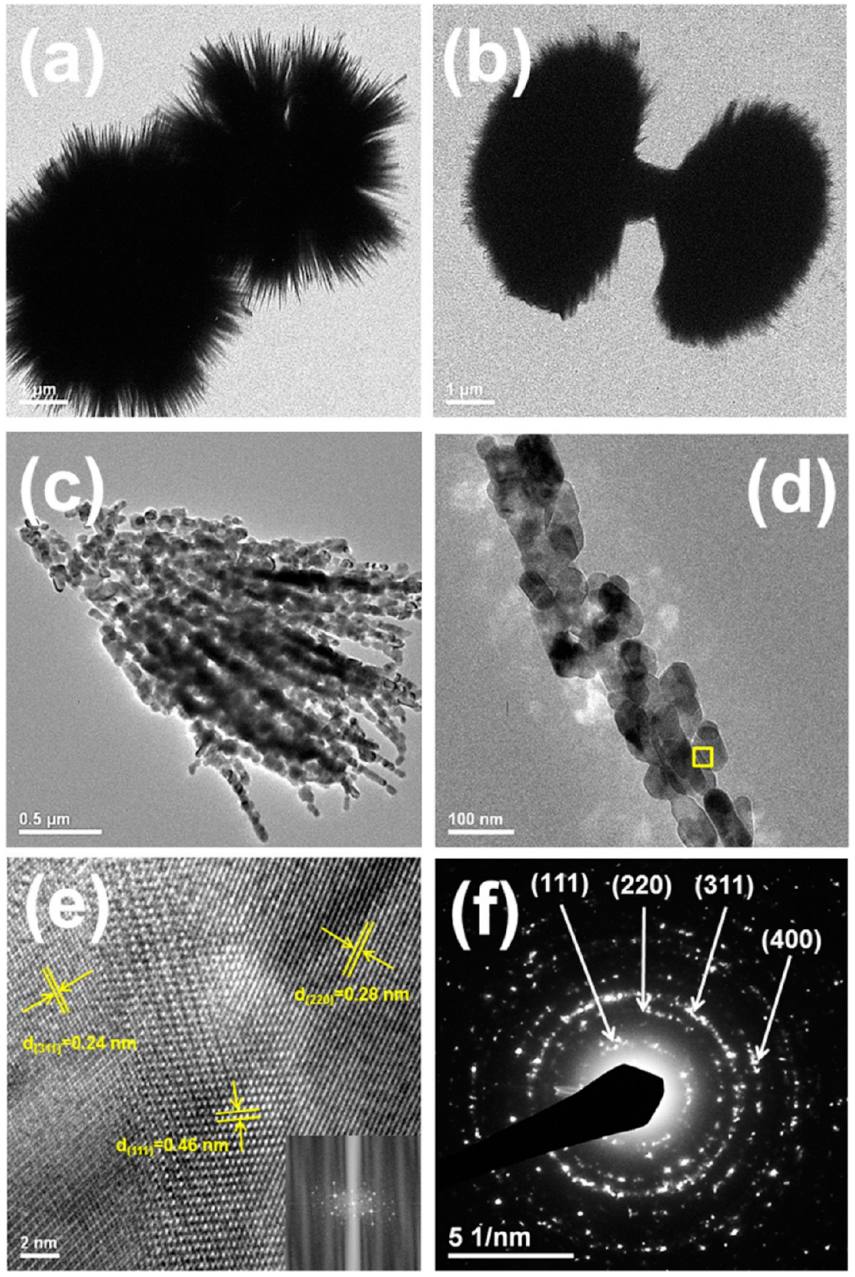

Figure 6. (a and b) Low-magnification TEM images of Co_3O_4 microsphere and microdumbbell, respectively. (c) TEM image of Co_3O_4 nanowire bundle obtained by sonication. (d) TEM image of a representative nanowire consisting of Co_3O_4 nanoparticles. (e) HRTEM image of area indicated by the yellow square in panel d, and (f) SAED images of primary Co_3O_4 nanoparticles.

behavior. The diameters of the semicircular loops of the EIS curves for the Co_3O_4 microdumbbell, microsphere, and nanocube electrodes are about 0.45, 0.51, and 0.75 Ω, respectively. This clearly illustrates that microdumbbell and microsphere structures have a better charge transport property than nanocubes. On top of that, the slope of straight segment of Co_3O_4 nanocube electrode is less than 45°, indicating that the material may not store electrochemical energy efficiently. Similar argument suggests that microdumbbell and microsphere are more suitable for supercapacitor electrode materials. On top of that, the slope of Co_3O_4 in lower frequency region microdumbbell electrode is higher than that of microsphere electrode, implying that dumbbell structure can result in better electrolyte diffusion.

CONCLUSIONS

In this paper, cobalt oxide, Co_3O_4, with different structures such as dumbbell, sphere, and cube has been synthesized. The main aim of this study is to design three-dimensional architecture electrode by combining the desired properties of microstructures and nanoscale building blocks. All electrodes fabricated from Co_3O_4 microstructures demonstrate surprisingly excellent long-term electrochemical stability in alkaline electrolyte, which fulfills our major goal. We also highlight the intriguing formation mechanism of cobalt precursor microdumbbell with addition of Co_3O_4 nanocubes in reaction mixture. It is postulated that modified Ostwald ripening and Kirkendall effects are responsible for the generation of this special 3D microstructure.

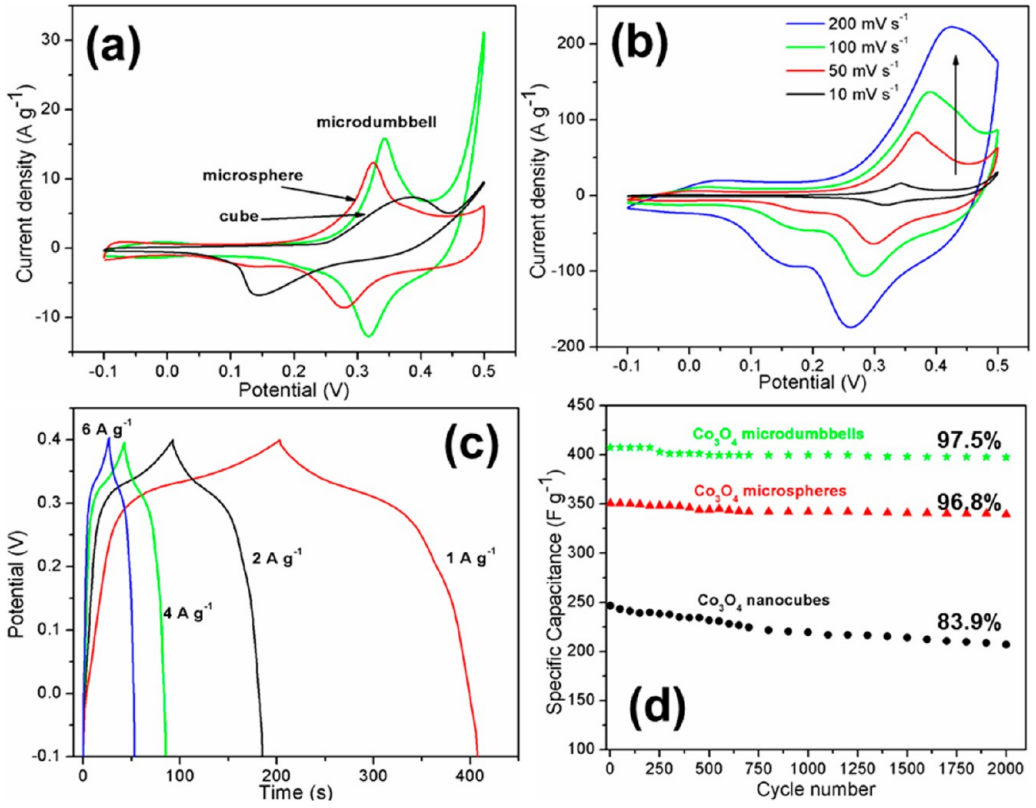

Figure 7. Electrochemical measurements. (a) Cyclic voltammograms (CVs) of Co_3O_4 microdumbbells, microspheres and nanocubes in 6 M KOH at 10 mV s^{-1}. (b) CVs of Co_3O_4 microdumbbells at various potential scan rates. (c) Galvanostatic charge−discharge curves of Co_3O_4 microdumbbell at different current densities. (d) Cycle life as-prepared Co_3O_4 with various structures in 6 M KOH electrolyte at 1 A g^{-1}.

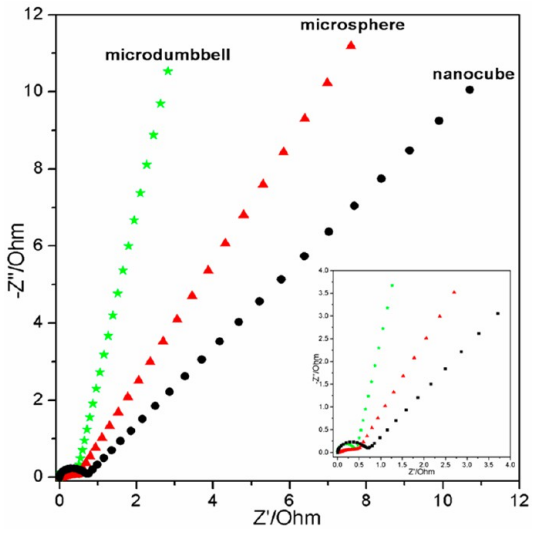

Figure 8. Complex-plane impedance spectra of the Co_3O_4 microdumbbell, microsphere, and nanocube electrodes. The inset is the enlarged image of spectra in the range from 0−4 ohm.

■ ASSOCIATED CONTENT

Ⓢ Supporting Information

Additional graphical representation of as-prepared nanostructures and electrochemical performance. This material is available free of charge via the Internet at http://pubs.acs.org.

■ AUTHOR INFORMATION

Corresponding Author

*J.-M. Lee. Tel.: +65 651 381 29. E-mail: jmlee@ntu.edu.sg.

Notes

The authors declare no competing financial interest.

■ ACKNOWLEDGMENTS

This work is supported by Academic Research Fund (RGT27/13) of Ministry of Education in Singapore.

■ REFERENCES

(1) Conway, B. E. Transition from "Supercapacitor" to "Battery" Behavior in Electrochemical Energy Storage. *J. Electrochem. Soc.* **1991**, *138*, 1539−1548.

(2) Conway, B. E. *Electrochemical Supercapacitors: Scientific Fundamentals and Technological Applications*; Kluwer Academic/Plenum Publishers: New York, 1999.

(3) Simon, P.; Gogotsi, Y. Materials for Electrochemical Capacitors. *Nat. Mater.* **2008**, *7*, 845−854.

(4) Salunkhe, R. R.; Jang, K.; Lee, S.-W.; Yu, S.; Ahn, H. Binary Metal Hydroxide Nanorods and Multi-walled Carbon Nanotube Composites for Electrochemical Energy Storage Applications. *J. Mater. Chem.* **2012**, *22*, 21630−21635.

(5) Dam, D. T.; Wang, X.; Lee, J.-M. Fabrication of Mesoporous $Co(OH)_2$/ITO Nanowire Composite Electrode and Its Application in Supercapacitors. *RSC Adv.* **2012**, *2*, 10512−10518.

(6) Rakhi, R. B.; Chen, W.; Cha, D.; Alshareef, H. N. Substrate Dependent Self-Organization of Mesoporous Cobalt Oxide Nanowires with Remarkable Pseudocapacitance. *Nano Lett.* **2012**, *12*, 2559−2567.

(7) Shim, H.-W.; Lim, A.-H.; Kim, J.-C.; Jang, E.; Seo, S.-D.; Lee, G.-H.; Kim, T. D.; Kim, D.-W., Scalable One-Pot Bacteria-Templating

Synthesis Route toward Hierarchical, Porous-Co_3O_4 Superstructures for Supercapacitor Electrodes. *Sci. Rep.* **2013**, *3*.
(8) Dam, D. T.; Lee, J.-M. Polyvinylpyrrolidone-Assisted Polyol Synthesis of NiO Nanospheres Assembled From Mesoporous Ultrathin Nanosheets. *Electrochim. Acta* **2013**, *108*, 617−623.
(9) Dam, D. T.; Wang, X.; Lee, J.-M. Mesoporous ITO/NiO with a Core/Shell Structure for Supercapacitors. *Nano Energy* **2013**, *2*, 1303−1313.
(10) Kwon, O. S.; Kim, T.; Lee, J. S.; Park, S. J.; Park, H.-W.; Kang, M.; Lee, J. E.; Jang, J.; Yoon, H. Fabrication of Graphene Sheets Intercalated with Manganese Oxide/Carbon Nanofibers: Toward High-capacity Energy Storage. *Small* **2013**, *9*, 248−254.
(11) Ye, Y.; Jo, C.; Jeong, I.; Lee, J. Functional Mesoporous Materials for Energy Applications: Solar Cells, Fuel Cells, and Batteries. *Nanoscale* **2013**, *5*, 4584−4605.
(12) Dam, D. T.; Lee, J.-M. Capacitive Behavior Of Mesoporous Manganese Dioxide On Indium−Tin Oxide Nanowires. *Nano Energy* **2013**, *2*, 933−942.
(13) Dam, D. T.; Lee, J.-M. Ultrahigh Pseudocapacitance of Mesoporous Ni-Doped $Co(OH)_2$/ITO Nanowires. *Nano Energy* **2013**, *2*, 1186−1196.
(14) Salunkhe, R. R.; Jang, K.; Lee, S.-W.; Ahn, H. Aligned Nickel-Cobalt Hydroxide Nanorod Arrays for Electrochemical Pseudocapacitor Applications. *RSC Adv.* **2012**, *2*, 3190−3193.
(15) Oh, E.-J.; Kim, T. W.; Lee, K. M.; Song, M.-S.; Jee, A.-Y.; Lim, S. T.; Ha, H.-W.; Lee, M.; Choy, J.-H.; Hwang, S.-J. Unilamellar Nanosheet of Layered Manganese Cobalt Nickel Oxide and Its Heterolayered Film with Polycations. *ACS Nano* **2010**, *4*, 4437−4444.
(16) Keng, P. Y.; Bull, M. M.; Shim, I.-B.; Nebesny, K. G.; Armstrong, N. R.; Sung, Y.; Char, K.; Pyun, J. Colloidal Polymerization of Polymer-Coated Ferromagnetic Cobalt Nanoparticles into Pt-Co_3O_4 Nanowires. *Chem. Mater.* **2011**, *23*, 1120−1129.
(17) Duay, J.; Sherrill, S. A.; Gui, Z.; Gillette, E.; Lee, S. B. Self-Limiting Electrodeposition of Hierarchical MnO_2 and $M(OH)_2/MnO_2$ Nanofibril/Nanowires: Mechanism and Supercapacitor Properties. *ACS Nano* **2013**, *7*, 1200−1214.
(18) Dam, D. T.; Wang, X.; Lee, J.-M. Graphene/NiO Nanowires: Controllable One-Pot Synthesis and Enhanced Pseudocapacitive Behavior. *ACS Appl. Mater. Interfaces* **2014**, *6*, 8246−8256.
(19) Song, M.-S.; Lee, K. M.; Lee, Y. R.; Kim, I. Y.; Kim, T. W.; Gunjakar, J. L.; Hwang, S.-J. Porously Assembled 2D Nanosheets of Alkali Metal Manganese Oxides with Highly Reversible Pseudocapacitance Behaviors. *J. Phys. Chem. C* **2010**, *114*, 22134−22140.
(20) Woo, M. A.; Song, M.-S.; Kim, T. W.; Kim, I. Y.; Ju, J.-Y.; Lee, Y. S.; Kim, S. J.; Choy, J.-H.; Hwang, S.-J. Mixed Valence Zn-Co-Layered Double Hydroxides and Their Exfoliated Nanosheets with Electrode Functionality. *J. Mater. Chem.* **2011**, *21*, 4286−4292.
(21) Lee, B.-S.; Son, S.-B.; Park, K.-M.; Lee, G.; Oh, K. H.; Lee, S.-H.; Yu, W.-R. Effect of Pores in Hollow Carbon Nanofibers on Their Negative Electrode Properties for a Lithium Rechargeable Battery. *ACS Appl. Mater. Interfaces* **2012**, *4*, 6702−6710.
(22) Wu, M.-S.; Huang, K.-C. Fabrication of Nickel Hydroxide Electrodes With Open-ended Hexagonal Nanotube Arrays for High Capacitance Supercapacitors. *Chem. Commun.* **2011**, *47*, 12122−12124.
(23) Koo, B.; Xiong, H.; Slater, M. D.; Prakapenka, V. B.; Balasubramanian, M.; Podsiadlo, P.; Johnson, C. S.; Rajh, T.; Shevchenko, E. V. Hollow Iron Oxide Nanoparticles for Application in Lithium Ion Batteries. *Nano Lett.* **2012**, *12*, 2429−2435.
(24) Titirici, M.-M.; Antonietti, M.; Thomas, A. A Generalized Synthesis of Metal Oxide Hollow Spheres Using a Hydrothermal Approach. *Chem. Mater.* **2006**, *18*, 3808−3812.
(25) Yang, L.; Cheng, S.; Ding, Y.; Zhu, X.; Wang, Z. L.; Liu, M. Hierarchical Network Architectures of Carbon Fiber Paper Supported Cobalt Oxide Nanonet for High-Capacity Pseudocapacitors. *Nano Lett.* **2011**, *12*, 321−325.
(26) Kim, J. S.; Shin, S. S.; Han, H. S.; Oh, L. S.; Kim, D. H.; Kim, J.-H.; Hong, K. S.; Kim, J. Y. 1-D Structured Flexible Supercapacitor Electrodes with Prominent Electronic/Ionic Transport Capabilities. *ACS Appl. Mater. Interfaces* **2013**, *6*, 268−274.
(27) Kim, J.-Y.; Kim, K.-H.; Kim, H.-K.; Park, S.-H.; Chung, K. Y.; Kim, K.-B. Nanosheet-assembled 3D Nanoflowers of Ruthenium Oxide with Superior Rate Performance for Supercapacitor Applications. *RSC Adv.* **2014**, *4*, 16115−16120.
(28) Xie, X.; Li, Y.; Liu, Z.-Q.; Haruta, M.; Shen, W. Low-Temperature Oxidation of CO Catalysed by Co_3O_4 Nanorods. *Nature* **2009**, *458*, 746−749.
(29) Wu, T.; Li, J.; Hou, L.; Yuan, C.; Yang, L.; Zhang, X. Uniform Urchin-like Nickel Cobaltite Microspherical Superstructures Constructed By One-Dimension Nanowires and their Application for Electrochemical Capacitors. *Electrochim. Acta* **2012**, *81*, 172−178.
(30) Liu, B.; Zhang, J.; Wang, X.; Chen, G.; Chen, D.; Zhou, C.; Shen, G. Hierarchical Three-Dimensional $ZnCo_2O_4$ Nanowire Arrays/Carbon Cloth Anodes for a Novel Class of High-Performance Flexible Lithium-Ion Batteries. *Nano Lett.* **2012**, *12*, 3005−3011.
(31) Xiao, J.; Yang, S. Sequential Crystallization of Sea Urchin-like Bimetallic (Ni, Co) Carbonate Hydroxide and Its Morphology Conserved Conversion to Porous $NiCo_2O_4$ Spinel for Pseudocapacitors. *RSC Adv.* **2011**, *1*, 588−595.
(32) Wu, F. D.; Wang, Y. Self-Assembled Echinus-like Nanostructures of Mesoporous CoO Nanorod@CNT for Lithium-Ion Batteries. *J. Mater. Chem.* **2011**, *21*, 6636−6641.
(33) Pang, H.; Zhang, B.; Du, J.; Chen, J.; Zhang, J.-S.; Li, S.-J. Porous Nickel Oxide Nanospindles with Huge Specific Capacitance and Long-Life Cycle. *RSC Adv.* **2012**, *2*, 2257−2261.
(34) Li, S.-H.; Qi, L.; Lu, L.-H.; Wang, H.-Y. Cotton-Assisted Preparation of Mesoporous Manganese Oxide for Supercapacitors. *RSC Adv.* **2012**, *2*, 6741−6743.
(35) Ge, X.; Gu, C. D.; Wang, X. L.; Tu, J. P. Correlation between Microstructure and Electrochemical Behavior of the Mesoporous Co_3O_4 Sheet and Its Ionothermal Synthesized Hydrotalcite-like α-$Co(OH)_2$ Precursor. *J. Phys. Chem. C* **2014**, *118*, 911−923.